Korean J. Chem. Eng., **30**(6), 1213-1221 (2013)
DOI: 10.1007/s11814-013-0028-5

Optimal oxygen concentration strategy through an isothermal oxidative coupling of methane plug flow reactor to obtain a high yield of C_2 hydrocarbons

Amideddin Nouralishahi*,*, Hassan Pahlavanzadeh**,†, Mohammadmehdi Choolaei***, Elaheh Esmaeili*, and Amir Yadegari*,***

*Catalysis and Nanostructured Materials Research Laboratory, School of Chemical Engineering, University of Tehran, P. O. Box 11155/4563 Tehran, Iran
**Chemical Engineering Department, Tarbiat Modares University, Tehran, Iran
***Carbon Nanotechnology and Energy Institute, Tehran, Iran
(*Received 29 September 2012 • accepted 24 February 2013*)

Abstract−An optimal oxygen concentration trajectory in an isothermal OCM plug flow reactor for maximizing C_2 production was determined by the algorithm of piecewise linear continuous optimal control by iterative dynamic programming (PLCOCIDP). The best performance of the reactor was obtained at 1,085 K with a yield of 53.9%; while, at its maximum value, it only reached 12.7% in case of having no control on the oxygen concentration along the reactor. Also, the effects of different parameters such as reactor temperature, contact time, and dilution ratio (N_2/CH_4) on the yield of C_2 hydrocarbons and corresponding optimal profile of oxygen concentration were studied. The results showed an improvement of C_2 production at higher contact times or lower dilution ratios. Furthermore, in the process of oxidative coupling of methane, controlling oxygen concentration along the reactor was more important than controlling the reactor temperature. In addition, oxygen feeding strategy had almost no effect on the optimum temperature of the reactor. Finally, using the optimal oxygen strategy along the reactor has more effect on ethylene selectivity compared to ethane.

Key words: Oxidative Coupling of Methane (OCM), Modelling, Optimization, Reaction Engineering, Optimal Control

INTRODUCTION

Direct conversion of methane to ethylene via oxidative coupling of methane (OCM) has been an active research area in recent years [1]. It was suggested that for making OCM economically probable, the yield of C_2 hydrocarbons has to be more than 30%. However, it is difficult to reach yields higher than 25% in typical reactors, because an increase in methane conversion usually results in lower C_2 selectivity [2]. Due to the low yield of C_2^+ production, it is ineluctable to use catalysts in oxidative coupling of methane. In fact, it was observed in several studies that there was almost no conversion below 800 °C in the absence of catalyst, while elevated temperatures and pressures led to a high non-selective conversion of methane, in non-catalytic OCM reactors [3,4]. Since the first work on the OCM process by Keller and Bhasin [5], a wide variety of catalysts have appeared [6-8]. Perovskite-type oxides, represented by the general formula of ABO_3, were found to be very active and selective toward C_2^+ hydrocarbons [9]. Silica-supported sodium promoted manganese oxides have been extensively evaluated and become more prominent since the finding of the Na_2WO_4-Mn/SiO_2 system. Surface WO_4^{2-} tetrahedron was emphasized to be the essence of the oxidative coupling of methane over M-W-Mn/SiO_2 catalysts [10].

By using membrane reactors, it is possible to have high selectivity and conversion via controlling oxygen concentration as one of the most important parameters, affecting the performance of the OCM process. Lu and coworkers showed that a higher local ratio of methane to oxygen leads to a higher C_2 selectivity, while it lowers methane conversion [2]. Olivier et al. studied the modification of ionic oxygen-conducting membrane reactor for oxidative coupling of methane to higher hydrocarbons with three different catalytic surface modifications [11]. The results illustrated that it is possible to achieve a C_2-hydrocarbon yield of more than 18% by using a LaSr/CaO modified membrane reactor. Bhatia and co-workers compared the performance of oxidative coupling of methane (OCM) in a catalytic membrane reactor (CMR), catalytic packed bed reactor (PBR), and catalytic packed bed membrane reactor (PBMR) [12] with the result that the catalytic membrane reactor, with C_2^+ yield of 34.7%, had the best performance among all the three mentioned reactors. Some other studies have been conducted on the modeling and simulation of OCM reactors. Kundu et al. presented a mathematical modeling of a five-section countercurrent moving bed chromatographic reactor (SCMCR) for OCM process [13]. The proposed mathematical model demonstrated extremely good predictions for experimental results. Nakisa and co workers showed that CFD tools make it possible to implement the heterogeneous kinetic model even for high exothermic reactions such as oxidative coupling of methane [14]. Tye and coworkers developed a one-dimensional model for the oxidative coupling of methane over La_2O_3/CaO catalyst in a packed fixed bed reactor [15]. They observed that the maximum value of C_2 yield was obtained at 1,098 K. Also, there have been some works addressing optimization techniques in OCM process, as well. For example, Istadi et al. developed an optimization of process parameters and catalyst compositions for the CO_2 oxidative coupling of methane over CaO-MnO/CeO_2 catalyst using response surface methodology (RSM) and reported maximum selectivity and

†To whom correspondence should be addressed.
E-mail: pahlavzh@modares.ac.ir

yield of 82.62% and 3.93% for C_2 hydrocarbons [16]. Amin et al. studied the effects of operating temperature, inlet oxygen concentration, and F/W on ethylene production in an OCM process over Li/MgO (Li/Mg=0.1) catalyst [17]. Numerical results indicated that the maximum value of ethylene yield was 8.14% at optimum operating temperature and oxygen concentration. Kundu et al. found that in an OCM reaction the performance of the simulated countercurrent moving bed chromatographic reactor (SCMCR) could be significantly improved under optimal operating conditions [18].

However, only few researches have addressed optimal control in the OCM process. Rojnuckarin et al. applied an optimal control strategy to the problem of finding the flux profiles for the conversion of methane to ethylene and acetylene in a plug flow reactor [19]. Faliks and co-workers applied an optimal methodology in a non-catalytic homogeneous gas phase conversion of methane to ethylene [20]. Also, in our previous work, we used the algorithm of piecewise linear continuous optimal control by iterative dynamic programming (PLCOCIDP) [21] to obtain optimal temperature trajectory in an OCM plug flow reactor. In addition, the effects of pressure and initial dilution ratio were studied on the final amount of ethylene production, as the objective function [22]. In the present study, we have compared the role of oxygen and temperature as two important variables in the OCM process. At first, with the aim of maximizing C_2 production, the optimal oxygen concentration strategy was obtained along a modeled OCM plug flow reactor [15] over La_2O_3/CaO catalyst particles using the algorithm of PLCOCIDP. Then, the effect of different parameters on the reactor performance was studied and the results were explained from chemical reactions point of view. Also, the level of improvement under the mentioned conditions was compared to the best performance of the reactor with the optimum dilution ratio without any side feeding streams.

In the current article, we assumed that the reactor operates under isothermal conditions. However, in highly exothermic reactions, such as OCM, the presence of hot spots on the surface of the catalyst particles is one of the major problems. The presence of hot spots decreases the catalyst life and leads to an unsatisfactory reactor yield. Also, they can be very hazardous at elevated operating temperatures. Hot spots usually occur when the rate of reaction is significantly high but there is a poor condition to remove the produced heat from the surface of the catalyst particles.

Several ways have been suggested to control hotspots along catalytic fixed bed reactors. One way to avoid hot spots is the injection of an inert gas with high specific thermal capacity (Cp), such as N_2, into the feeding streams [23]. Dilution of reactants with an inert gas stream results in a decrease in the amount of produced heat per unit volume of rector. Moreover, the high value of Cp makes it possible to avoid undesirable temperature enhancement on the surface of the catalyst active sites.

Moreover, it can be advantageous to apply inert particles, such as glass beads, accompanied with catalyst particles in sections with high probability of hot spot formation, i.e., sections in which the rate of heat generation is remarkably high. The presence of inert particles could decrease the produced heat per unit volume, which makes it easy to control temperature along the reactor [24].

In addition, a wall-cooled tubular reactor design could be suitable for controlling the generated heat, to keep the temperature profile uniform along the reactor. Karafyllis and Daoutidis have shown that the magnitude of hot spots in plug flow reactors could be extremely suppressed by manipulating the temperature of the jacket coolant through a nonlinear control procedure [25].

1. The Reaction Scheme

Instead of complicated radical reaction schemes used by other researchers [19,20], we applied a simple ten step molecular mechanism with proper accuracy [26] for predicting the reactor conditions. The used reaction network consists of nine heterogeneous and one homogeneous reaction steps. According to this model, methane may be converted within three parallel reactions: (1) to ethane by an oxidative coupling reaction, (2) to CO_2 via nonselective total oxidation, and (3) to CO through a partial oxidation reaction. In consecutive steps, ethane may be converted to ethylene by heterogeneous catalytic oxidative dehydrogenation and/or thermal gas-phase dehydrogenation reaction. The used reaction scheme, proposed by Stansch et al. [27], is presented as follows:

$$CH_4+2O_2 \rightarrow CO_2+2H_2O \quad (1)$$

$$2CH_4+0.5O_2 \rightarrow C_2H_6+H_2O \quad (2)$$

$$CH_4+O_2 \rightarrow CO+H_2O+H_2 \quad (3)$$

$$CO+0.5O_2 \rightarrow CO_2 \quad (4)$$

$$C_2H_6+0.5O_2 \rightarrow C_2H_4+H_2O \quad (5)$$

$$C_2H_4+2O_2 \rightarrow 2CO+2H_2O \quad (6)$$

Table 1. The kinetic parameters [27]

Step	$K_{0,j}$ ($mol \cdot g^{-1} \cdot s^{-1} \cdot Pa^{-(m+n)}$)	$E_{a,j}$ ($kJ \cdot mol^{-1}$)	m_j	n_j	$K_{j,CO2}$ (Pa^{-1})	$\Delta H_{ad,CO2}$ ($kJ \cdot mol^{-1}$)	$K_{j,O2}$ (Pa^{-1})	$\Delta H_{ad,O2}$ ($kJ \cdot mol^{-1}$)
1	0.20×10^{-5}	48	0.24	0.76	0.25×10^{-12}	−175		
2	23.2	182	1.0	0.40	0.83×10^{-13}	−186	0.23×10^{-11}	−124
3	0.52×10^{-6}	68	0.57	0.85	0.36×10^{-13}	−187		
4	0.11×10^{-3}	104	1.0	0.55	0.40×10^{-12}	−168		
5	0.17	157	0.95	0.37	0.45×10^{-12}	−166		
6	0.06	166	1.0	0.96	0.16×10^{-12}	−211		
7	1.2×10^{-7}[a]	226						
8	9.3×10^{3}	300	0.97	0				
9	0.19×10^{-3}	173	1.0	1.0				
10	0.26×10^{-1}	220	1.0	1.0				

[a]Units are $mol \cdot s^{-1} \cdot m^{-3} \cdot Pa^{-1}$

Table 2. Allowable range of selected reaction scheme [27]

M_{cat}/V_{STP} (kg·s/m^3)	P_{tot} (kPa)	P^o_{O2} (kPa)	P^o_{CH4} (kPa)	T (K)	Process conditions
7.6×10^{-1}-250	100-130	1-20	10-95	973-1228	Range

$$C_2H_6 \rightarrow C_2H_4+H_2 \quad (7)$$

$$C_2H_4+2H_2O \rightarrow 2CO+4H_2 \quad (8)$$

$$CO+H_2O \rightarrow CO_2+H_2 \quad (9)$$

$$CO_2+H_2 \rightarrow CO+H_2O \quad (10)$$

To avoid hot spots in the reactor, nitrogen must be added to the inlet gas flow beside the above reactants. The estimated rates of the above reactions can be given by Eqs. (11)-(16) [27]. The kinetic parameters in the reaction scheme and permitted ranges for the state variables (temperature, pressure and concentrations) and the control variable (local concentration of O_2) are presented in Tables 1 and 2 [27], respectively.

$$r_j=(k_{0,j}e^{-E_{a,j}/RT}P_c^{mj}P_{O2}^{nj})/(1+K_{jCO2}e^{-\Delta H_{ad,CO2}/RT}P_{CO2})^2 \qquad j=1, 3\text{-}6 \quad (11)$$

$$r_2=(k_{0,2}e^{-E_{a,2}/RT}(k_{0,O2}e^{-\Delta H_{ad,O2}/RT}P_{O2})^n{}_2\,P_{CH4})/[(1+K_{jO2}e^{-\Delta H_{ad,O2}/RT}P_{O2})^n{}_2 + K_{jCO2}e^{-\Delta H_{CO2}/RT}P_{CO2}]^2 \quad (12)$$

$$r_7=k_{0,7}e^{-E_{a,7}/RT}P_{C2H6} \quad (13)$$

$$r_8=k_{0,8}e^{-E_{a,8}/RT}P_{C2H4}{}^{m8}P_{H2O}{}^{n8} \quad (14)$$

$$r_9=k_{0,9}e^{-E_{a,9}/RT}P_{CO}{}^{m9}P_{H2O}{}^{n9} \quad (15)$$

$$r_{10}=k_{0,10}e^{-E_{a,10}/RT}P_{CO2}{}^{m10}P_{H2}{}^{n10} \quad (16)$$

2. Theory

We have used the modeling equations proposed by Tye et al. [15]. These equations were resolved in our previous work [22] and were verified by comparing with the experimental [23] and simulated results [15]. To model the plug follow reactor, the following assumptions were made: (a) steady state one-dimensional plug flow, (b) immediate radial mixing, (c) no diffusion along the reactor axis, and (d) isothermal reaction conditions. To make the hypotheses practical, the ratio of the length of the reactor to its radius was selected to be higher than 25 [20]. However, since it is assumed that all reactions take place at isothermal conditions, there is no necessity to solve energy balance equation along the reactor. As well, it is not useful to write a mass balance equation for oxygen, because its concentration is selected as the control variable. Therefore, the differential equations set of the reactor consists of seven mass balance equations and a correlation for momentum balance (Ergun equation) which are presented as follows:

Table 3. The reactor and model parameters

Length of reactor (m)	2
Diameter of the reactor (m)	0.05
Initial volumetric flow at standard conditions (lit/s)	3
Contact time (kg.s/(m^3))	20-250
Packing diameter (m)	0.0125
Porosity	0.5317
Pressure (bar)	1.3
Weight of the applied catalyst (g)	60-250

Mass balance: $d(C_i)/d(Z)=1/U_s(\varepsilon_b\Sigma\alpha_{i,j}r_{g,j}+\rho_b\Sigma\alpha_{i,j}r_{c,j})$ (17)

Momentum balance:

$$d(P)/d(Z)=-(\rho_g U_s^2/\psi d_p)[(150(1-\varepsilon_b)/\psi Re)+1.75]\,(150(1-\varepsilon_b)/\varepsilon_b) \quad (18)$$

The boundary conditions and reactor structural characteristics required for solving the above modeling equations (Eqs. (17) and (18)) have been given in Table 3. According to this table, the porosity is considered to be fixed at 0.5317 while the amount of applied catalysts varies during the current research. Since the value of porosity severely depends on the amount of applied particles in the catalytic bed, it is assumed that the catalyst particles are mixed with inert quartz beads in such a way that the porosity remains unchanged. Furthermore, the presence of inert particles in catalytic bed may be helpful for avoiding hot spots along the reactor [24].

For achieving the optimal profile of oxygen concentration along the reactor, it is supposed that it is possible to control oxygen concentration (as the control variable) at each segment by considering an oxygen feeding policy. From a practical point of view, it may be possible to control oxygen concentration along the reactor by using some feeding side streams (Fig. 1).

Since the performance index (P.I) in this work is to maximize C_2 production, the related objective function is introduced as ethylene and ethane molar flux at the end of the reactor (Eq. (19)).

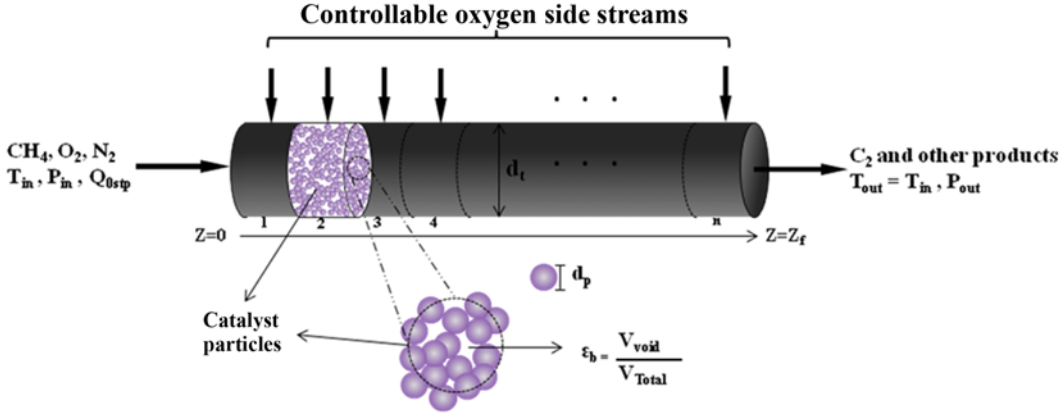

Fig. 1. Schematic reactor with several feeding side streams to control local oxygen concentrations.

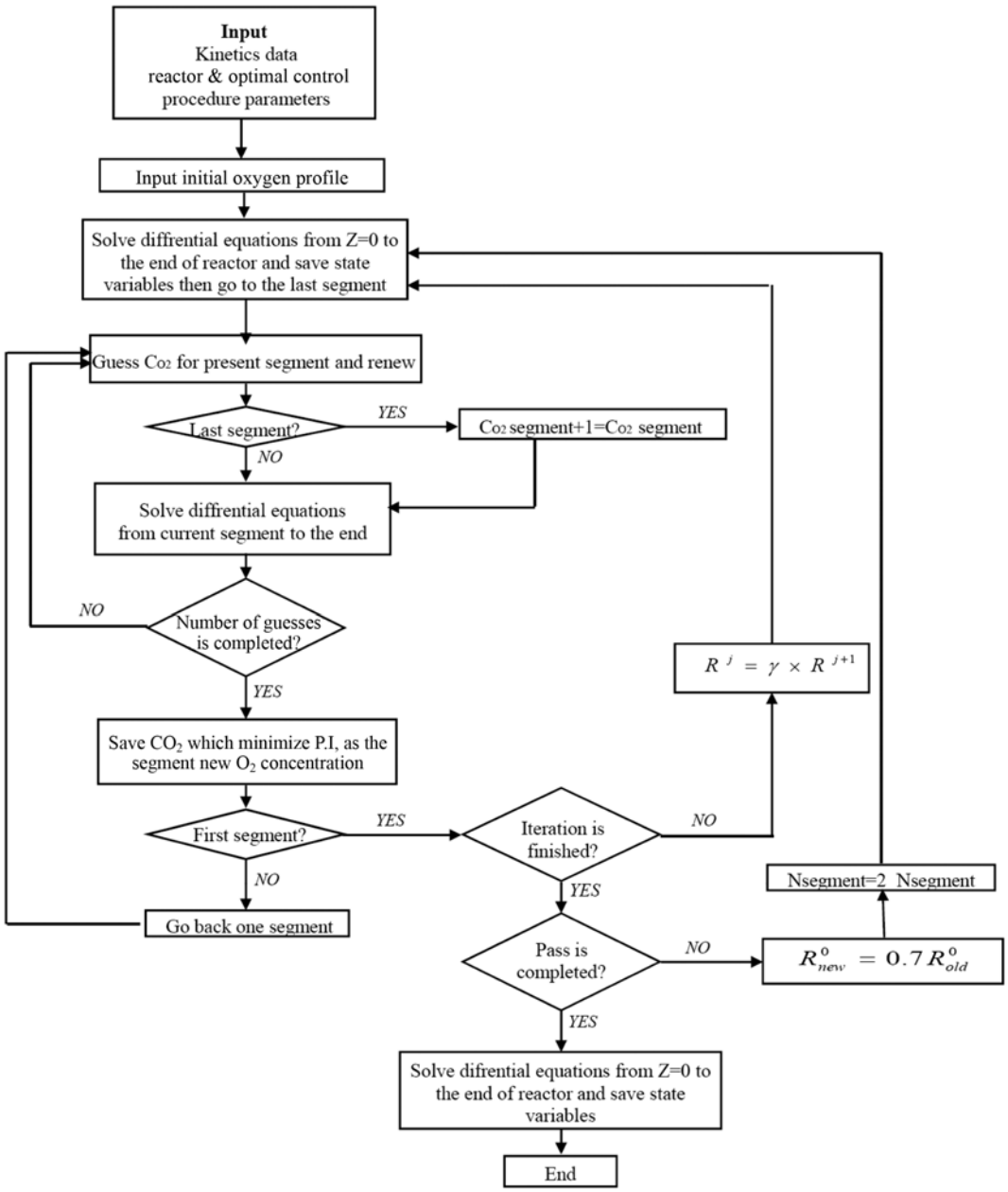

Fig. 2. Schematic algorithm of PLCOCIDP for obtaining maximum C_2 production in OCM plug flow reactor.

$$P.I.=(u_s(C_{C2H4}+C_{C2H6}))_{Z=Zf} \quad (19)$$

Because oxygen concentration is selected as the control variable, O_2 concentration at each segment must be changed in such a way that the performance index gets its maximum value. As a result, it is necessary to renew mass balance equations and calculate the new concentration value of all species at each segment. Fig. 2 shows the schematic algorithm of piecewise Linear continuous optimal control by iterative dynamic programming (PLCOCIDP) in case of determining optimal trajectory of oxygen concentration along the reactor.

We decided to use a multi-pass method where the number of segments was doubled after every pass, each consisting of 30 iterations, and the best obtained oxygen concentration was used as an initial oxygen concentration for the next pass. Also, the initial uniform oxygen concentration of 0.4 (mole/m^3) was selected as the initial guess for the optimal concentration profile, in all cases.

Fig. 3 shows the performance index, calculated by Eq. (17), at each iteration within the last pass, at P_t=130 kPa and y^o_{O2}=0.15. As it is shown, the performance index rapidly increases from 7.085 (mole/m^2·s) to 7.3448 (mole/m^2·s) and then remains constant to the end. Although global optimality could not be guaranteed, Fig. 3 proves that high-quality solutions were obtained using the selected algorithm.

RESULTS AND DISCUSSION

Fig. 4(a) shows the optimal oxygen profile across the reactor at different dilution ratios. In this figure, it is obvious that there are

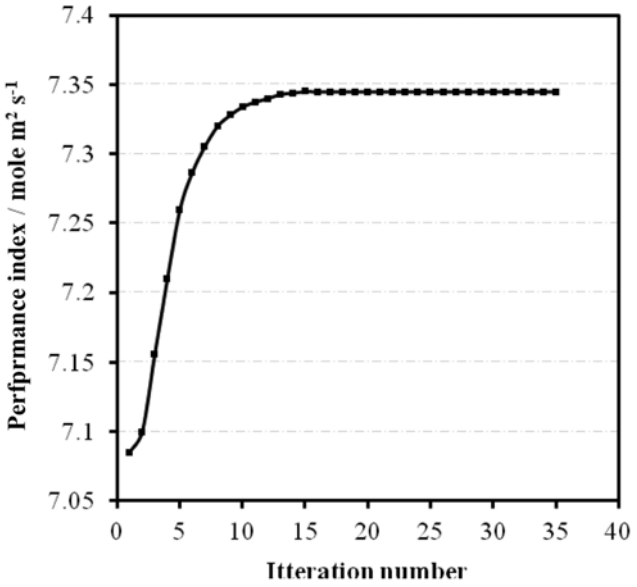

Fig. 3. Convergence of the purposed algorithm.

two different regions in all cases. In the first quarter of the reactor, the oxygen concentration decreases dramatically and after that, in the second part, it remains steady until the end.

Since, at the beginning of the reactor just methane and oxygen exist as reactants, only reactions 1, 2, and 3 can take place. Because in Eq. (12), the amount of $K_{0,2}$ is much higher than $K_{0,1}$ and $K_{0,3}$, in Eq. (11), a small change in the oxygen partial pressure (oxygen concentration) in the reactor has greater influence on the rate of reaction 2 compared to reactions 1 and 3. Therefore, the former reaction is more sensitive to oxygen partial pressure in comparison with the two other reactions. Hence, raising the concentration of oxygen at the beginning causes higher production of ethane with a higher rate than carbon oxides. Also, at higher dilution ratios, the initial oxygen concentration should be lowered to avoid C_2H_6 burning by oxidation reactions. Keeping high O_2 concentration in the rest of the reactor raises the rate of reactions 4 and 6, which results in ethylene consumption and consequently enhancing CO_2 production. On the other hand, as can be seen in Eq. (12), the terms of carbon dioxide partial pressure appear in denominators; therefore, generally any increase in carbon dioxide diminishes C_2 producing reaction rates. Thus, the oxygen concentration should decline in such a way that the rates of all oxidation reactions are minimized and, simultaneously, the rate of C_2 production (through reaction 2) becomes reasonable. Lowering oxygen concentration along the reactor has a good agreement with the results published by Santamaria et al., who suggested low oxygen concentration at local points within a plug flow reactor, in order to maximize C_2 production [29].

As shown in Fig. 4(b), the best yield of C_2 production is 53.9%, which is related to the absence of N_2 in the feed stream. In fact, adding nitrogen at the inlet of the reactor causes a decrease in the concentration of CH_4, which results in a significant fall in the yield of ethane and ethylene due to the higher sensitivity of the second reaction (in the applied reaction network) to the methane concentration. However, some researchers have reported the positive effect of inert gas on the total yield and selectivity under isothermal conditions [30]. For example, Tye et al. reported an optimum value of 55% for nitrogen as the inert gas in feeding stream of a co-fed plug flow reactor with the catalyst of La_2O_3/CaO [15]. Based on their study, the increase in reactants conversion with raising the inert gas molar ratio was due to the dilution effect of oxygen, which encouraged the methane coupling reaction and suppressed the deep oxidations. However, since in the current study the oxygen stream is independently controlled at each segment of the reactor, it is not necessary to inject nitrogen, as a controller of oxygen concentration. On the other hand, from a practical point of view, nitrogen must be added to the reactant streams as a thermal moderator to avoid hot spots on the particle surfaces across the catalytic beds. Therefore, to improve the overall performance of an actual OCM plug flow reactor, the dilution ratio should be decreased as much as possible.

The effect of contact time (total amount of applied catalyst/initial methane mass flow rate) on the optimal oxygen profiles and corresponding final yields was also investigated. In Fig. 5(a), a decrease in contact time makes the oxygen profile to grow gradually. In fact, at lower contact time the undesirable side reactions are not able to take place adequately; therefore, local oxygen concentrations are able to reach higher amounts at the subsequent. In Fig. 5(b), the yield of C_2 production (ethane and ethylene) improves from 29.2% to 53.9% when the contact time is enhanced from 20 to 250 kg·s/m^3, respectively.

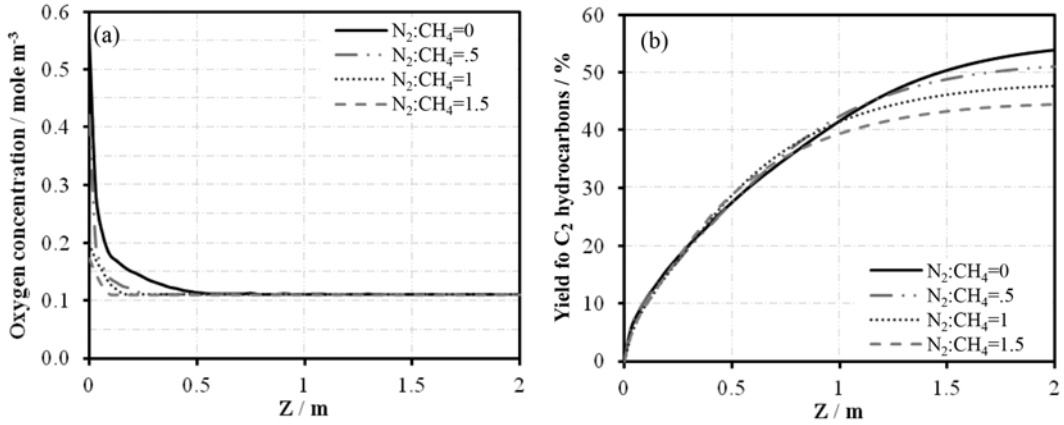

Fig. 4. Effect of Dilution ratio on optimal oxygen concentration profile (a) and corresponding C_2 production (b) at (P=1.3 bar and T= 1,085 K and contact time=250 kg·s/m^3).

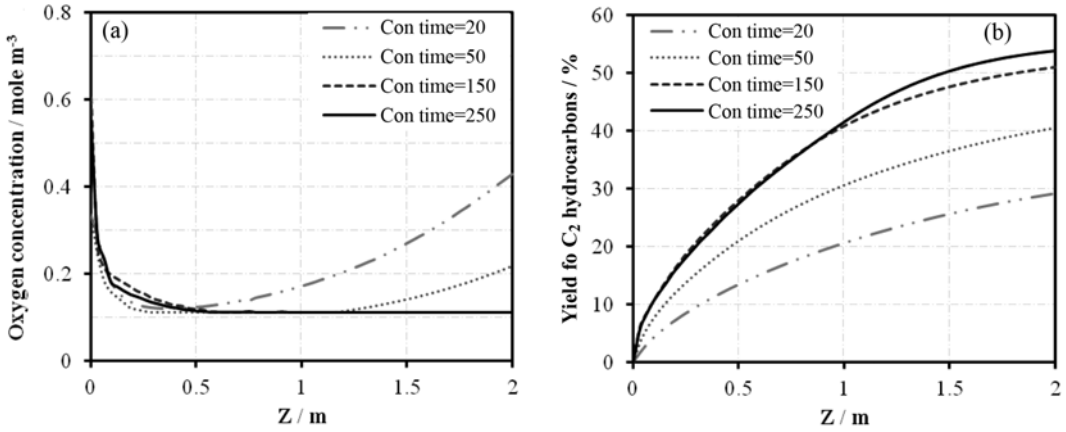

Fig. 5. Effect of contact time (kg·s/m^3) on optimal oxygen concentration profile (a) and corresponding C_2 production (b) at (P=1.3 bar and T=1,085 K and Dilution ratio=0).

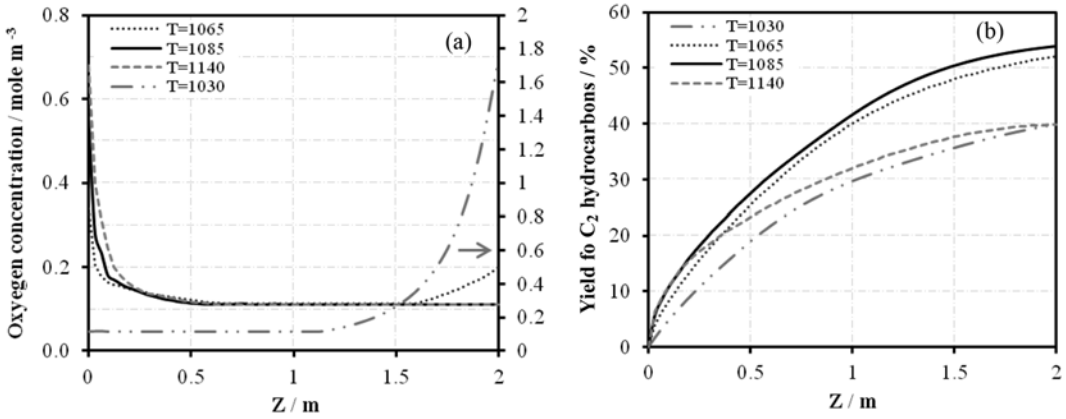

Fig. 6. Effect of temperature (K) on optimal oxygen concentration profile (a) and corresponding C_2 production at (P=1.3 bar and contact time=250 kg·s/m^3 and Dilution ratio=0).

As expected in catalytic reactions, an increase in contact time increases the rate of all reactions; therefore, the conversion of methane enhances, and consequently higher amounts of ethane and ethylene are produced. As a result, it can be concluded that oxidation coupling reaction (Eq. (2)) is more dependent on the amount of applied catalyst compared to other deep oxidation reactions. Also, since oxygen does not vanish in any segment, because of injected side streams, the yield of C_2 does not remain steady along the reactor [15].

Figs. 6(a) and 6(b), demonstrate the effects of temperature on the optimal oxygen profiles and corresponding C_2 production, respectively. The highest yield is obtained at optimum temperature of 1,085 K. In fact, at high temperatures the rate of undesirable reactions rises, and conversely low temperatures cannot supply the needed energy for useful reactions. At temperatures below 1,085 K the second part of oxygen profiles rises slightly. This can be explained by higher temperature and oxygen sensitivity of the second reaction (Eq. (2)), which leads to lower oxygen concentration at the beginning to compensate the negative effects of low temperature on ethane production. Subsequently, in the second part of the reactor the oxygen concentration can rise slightly with decreasing the rate of side reactions as a result of methane consumption. Also, interestingly, at very low temperatures (i.e., 1,030 K) the pattern of the oxygen optimal profile is totally inverted. As well, by comparing the optimum temperature (1,085 K) with the ones in previous works [15,22], it can be concluded that the oxygen feeding strategy has a negligible effect on the optimum isothermal temperature.

Fig. 7 compares the profiles of yield and selectivity of C_2 productions in case of applying the optimal oxygen concentration profile at 1,085 K. It appears in Fig. 7(a) that using the optimal oxygen concentration along the reactor causes a steady increase in ethylene production. On the other hand, the produced ethane in the first quarter is converted to other species in the rest of the reactor, which causes a decrease in the yield of ethane (see Fig. 7(a)). Consequently, it can be concluded that applying the optimal oxygen concentration strategy along the reactor poses the ethylene consumption to reduce as much as possible. In Fig. 7(b), due to the absence of other components and the high sensitivity of the second reaction to oxygen concentration, the selectivity of ethane shows a sudden increase at the beginning of the reactor where oxygen has a high concentration (Figs. 4(a), 5(a), and 6(a)). However, it experiences a dramatic drop-off in continuing because of reactions 5 and 7, which produce ethylene from ethane; therefore, the profile of ethylene selectivity shows a gradual increase along the reactor. On the other hand, because of ethylene consumption by reactions 8 and especially reaction 6, the ramp of ethylene selectivity reduces gradually, and finally

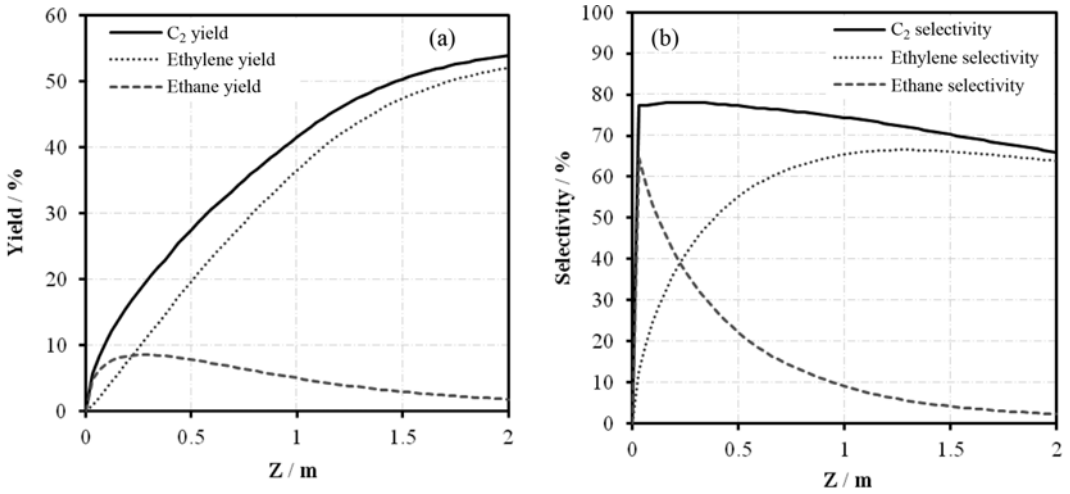

Fig. 7. The profiles of yield (a) and selectivity (b) for ethane, ethylene, and C_2 production along the reactor at 130 Kpa, 1,085 K, dilution ratio=0, and contact time=250 kg·s/m^3.

Table 4. The effect of operating conditions on the reactor overall performance

Reactor conditions	Methane conversion (%)	Yield of C_2H_4 (%)	Yield of C_2H_6 (%)	Yield of C_2 (%)	C_2 Selectivity (%)
The best co-fed reactor @ C.t.[a]=250, Dl. Ratio[b]=0 T=1,085 K	21.9	8.9	3.8	12.7	50.1
C.t.=250 dl. Ratio=0					
T=1,030 K	62.3	36.1	3.7	39.8	63.9
T=1,065 K	75.1	49.7	2.5	52.2	69.4
T=1,085 K	81.6	52.1	1.8	53.9	66
T=1,140 K	82.7	38.1	1.7	39.8	48.1
C.t.=250 T=1,085 K					
Dl. ratio=0.5	83.4	49.3	1.67	50.97	61.1
Dl. ratio=1	84.2	46	1.7	47.7	56.6
Dl. ratio=1.5	84.05	42.8	1.7	44.5	52.9
Dl. ratio=0 T=1,085 K					
C.t.=20	43.37	23.3	5.9	29.2	67.4
C.t.=50	57.7	36	4.54	40.54	70.3
C.t.=150	75.8	48.6	2.4	51	67.3

[a]Contact time (kg·s/m^3) (mass of catalyst)/(inlet volumetric flow rate at standard condition)
[b]Dilution ratio (N_2 molar ratio/CH_4 molar ratio)

in the last quarter it declines slowly. The graph of C_2 selectivity is indeed a summation of ethane and ethylene selectivity graphs. Accordingly, its sudden increase in Fig. 7(b) can be explained by ethane production from reaction 2, as mentioned above. As it appears in Fig. 7(b), the graph of C_2 selectivity almost remains steady in the first quarter. This clearly proves that at the first part of the reactor there is approximately no consumption of ethylene species. However, the graph shows a gradual decrease from the next quarter to the end as a result of reactions 6 and 8. These results explain why the oxygen concentration in Figs. 4(a), 5(a), and 6(a) declines severely, in the first quarter of the reactor, and subsequently it remains stable until the end.

The effect of reactor operating conditions on the overall performance is briefly shown in Table 4. It is clear that without any control on the oxygen concentration along the reactor, one can just reach the yield of 12.7% at the optimum initial oxygen concentration (2.2 mole/m^3). This is far less than the maximum reachable value with optimal oxygen policy at T=1,085 K with a contact time of 250 kg·s/m^3, and N_2/CH_4=0 (i.e. 53.9%). In fact, applying the oxygen optimal trajectory causes an increase of 324%, 31.7%, and 272% in the yield of C_2 production, C_2 selectivity, and methane conversion, respectively. These are relatively in contrast to results published by Androulakis and Reyes who proposed that the yield of C_2 production in oxidative coupling of methane over Sm_2O_3 shows only gradual improvements by the distribution of oxygen concentration [31]. The conflict may arise from differences in applied reaction schemes

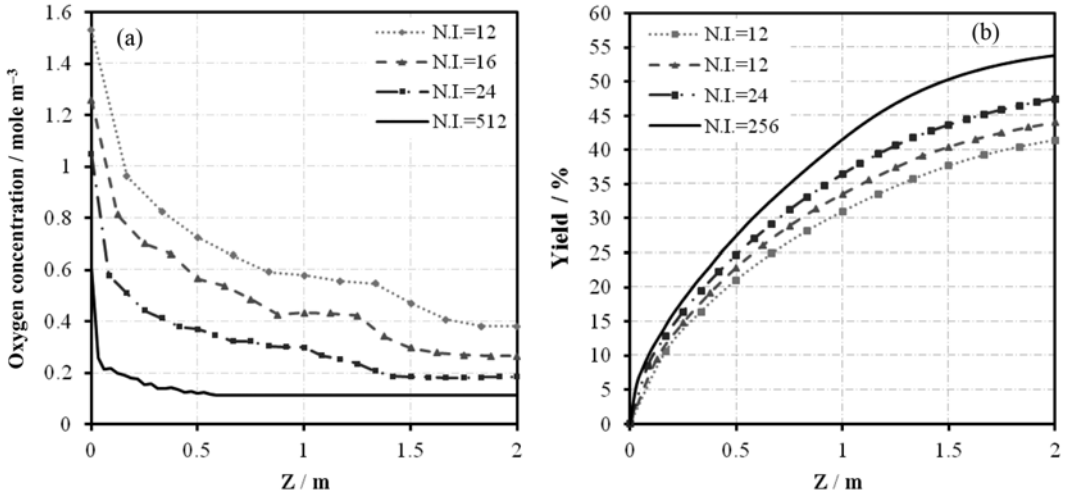

Fig. 8. Progress in optimal oxygen concentration profile at (P=1.3 bar and contact time=250 kg·s/m^3 and Dilution ratio=0) and the corresponding C2 yield with increasing number of injection points.

and the catalyst properties.

Based on Su and coworkers, the upper bound on OCM yield under conventional, packed-bed, co-fed operation can theoretically reach only 28%, at the optimum condition [32]. This shows that controlling the oxygen concentration is highly critical to make the OCM process economically feasible. In fact, according to our previous work [22], controlling oxygen concentration through an OCM reactor is more applicable and effective than controlling the temperature. Furthermore, according to Table 4, using an optimal oxygen strategy along the reactor leads to producing ethylene much more selectively than ethane in all cases, which can be very attractive economically. However, the type of the modeled reactor is very important to determine the overall OCM performance. It was shown that in a fluidized bed reactor of oxidative coupling of methane, the yield of products in stage-wise feeding, at high temperatures, is lower than co-feeding configuration [33], which is not in agreement with the reported results in our study. This may arise from differences between hydrodynamic conditions along the reactors, which cause some variations in the mixing state of reactant streams.

The results reported here are associated with a relative ideal case in which 512 injection points are considered along the reactor (N.I.= 512). However, the optimal oxygen concentration trajectory and the corresponding profiles of C_2 yield and selectivity are deeply dependent on the number of injection points of oxygen side streams along the reactor. The effect of increasing the number of injection points on the optimal oxygen concentration profile is presented in Fig. 8(a). Here, as a general trend, local oxygen concentration rises with decreasing the number of side streams along the reactor. This leads to a fall in the final C_2 yield (from 53.9% at N.I.=512 to 41.4% at N.I.=12), which is due to facilitation in kinetics of deep oxidation reactions (i.e., reactions 1, 3, and 6) in the presence of excess oxygen molecules (Fig. 8(b)). However, when the number of injection points increases from 12 to 24, the C_2 yield correspondingly improves from 41.4% to 47.4%, which is satisfactorily near to the final value (53.9%). This shows that although the optimal oxygen feeding strategy is very difficult to reach in a real case, it is still possible to achieve reasonable results by controlling oxygen profile through the reactor.

As a crucial conclusion from our study, more laboratory studies of oxidative coupling of methane still appear attractive to research, especially including optimal control to achieve the best possible performance.

CONCLUSION

An optimal profile of oxygen concentration in a fixed bed plug flow reactor of OCM process was obtained and the effects of different parameters such as dilution ratio (N_2/CH_4), contact time, and temperature were studied. The results showed an improvement in ethylene and ethane production at high contact times or low dilution ratios (N_2/CH_4). As a result, in the case of OCM reactors, it is better to lower inlet nitrogen flow rate as much as possible. Among all allowable optimal conditions, the best yield of almost 54% was obtained with a contact time of 250 kg·s/m^3, dilution ratio of zero (N_2/CH_4=0), and temperature of 1,085 K, while the best yield of co-fed reactor ,without any side streams, only reached 12.7% at its optimum condition. Also, oxygen feeding strategy almost had no effect on the reactor optimum operating temperature. In addition, using optimal oxygen strategy along the reactor led to a more selective production of ethylene compared to ethane. Finally, in an OCM process, controlling oxygen concentration along the reactor is more critical than controlling the reactor temperature.

NOMENCLATURE

C_i : molar concentration of component [mol/m^3]
$Cp_{ave.}$: specific heat capacity [kj/kg k]
$E_{a,j}$: activation energy in reaction j [kj/mol]
N.I. : number of injection points
P : total pressure of the system [kpa]
P_i : partial pressure of component I [KPa] kinetic parameter [Pa^{-1}]
P.I : performance index
R^0 : initial margin for guessing control variable
Re : Reynolds number
T : temperature [K]
U_s : superficial velocity [m/s]

Z : length [m]
Z_f : length of the reactor [m]
d_p : packing diameter [m]
d_t : reactor diameter [m]
$r_{c,I}$: rate of formation of catalytic reaction j [(mol i)/(m^2s)]
$r_{g,I}$: rate of formation of gas-phase reaction j [(mol i)/(m^2s)]
ΔH_j : heat of reaction j [kj/kg k]
q'' : heat of flux [kj/m^2s]
γ : reduction factor
ε_b : average porosity of bed
ρ_b : density of gas flow [kg/m^3]
$\alpha_{i,j}$: stoichiometric coefficient of component i in reaction j
ρ_b : density of catalyst in the bed [g/m^3]
ψ : shape factor

REFERENCES

1. W. T. Joris, S. Jianjun, O. Louis, C. V. André, M. Claude and B. M. Guy, *Catal. Today*, **159**, 29 (2011).
2. Y. Lu, A. G. Dixon, W. R. Moser and Y. H. Ma, *Chem. Eng. Sci.*, **55**, 4901 (2000).
3. M. Traykova, N. Davidova, J. Tsaih and A. H. Weiss, *Appl. Catal. A*, **169**, 237 (1998).
4. O. T. Onsager, R. Lodeng, P. Soraker, A. Anundskaas and B. Helleborg, *Catal. Today*, **4**, 355 (1989).
5. G. E. Keller and M. M. Bhasin, *J. Catal.*, **73**, 9 (1982).
6. J. S. Sung, K. Y. Choo, T. H. Kim, A. Greish, L. Glukhov, E. Finashina and L. Kustov, *Appl. Catal. A*, **380**, 28 (2010).
7. Z. Gholipour, A. Malekzadeh, R. Hatami, Y. Mortazavi and A. A. Khodadadi, *J. Nat. Gas Chem.*, **19**, 35 (2010).
8. J. S. Ahari, M. T. Sadeghi and S. Z. Pashne, *J. Taiwan Inst. Cheme. E*, **42**, 751 (2011).
9. N. R. Farooji, A. Vatanil and S. Mokhtari, *J. Nat. Gas Chem*., **19**, 385 (2010).
10. M. Ghiasi, A. Malekzadeh, S. Hoseini, Y. Mortazavi, A. Khodadadi and A. Talebizadeh, *J. Nat. Gas Chem.*, **20**, 428 (2011).
11. L. Olivier, S. Haag, C. Mirodatos, A. C. van Veen, *Catal. Today*, **142**, 34 (2009).
12. S. Bhatia, C. Y. Thien and A. Mohamed, *Chem. Eng. J.*, **148**, 525 (2009).
13. P. K. Kundu, Y. Zhang and A. K. Ray, *Chem. Eng. Sci.*, **64**, 5143 (2009).
14. N. Yaghobi and M. H. Ghoreishy, *J. Nat. Gas Chem.*, **18**, 39 (2009).
15. C. T. Tye, A. Mohamed and S. Bhatia, *Chem. Eng. J.*, **87**, 49 (2002).
16. I. Istadi and N. A. S. Amin, *Fuel Process. Technol.*, **87**, 449 (2006).
17. N. A. S. Amin and S. E. Pheng, *Chem. Eng. J.*, **116**, 187 (2006).
18. P. K. Kundu, Y. Zhang and A. K. Ray, *Chem. Eng. Sci.*, **64**, 4137 (2009).
19. A. Rojnuckarin, C. A. Floudas, H. Rabitz and R. A. Yetter, *Ind. Eng. Chem. Res.*, **35**, 683 (1996).
20. A. Faliks, R. A. Yetter, C. A. Floudas, R. Hall and H. Rabitz, *J. Phys. Chem. A*, **104**, 10740 (2000).
21. R. Luus and N. O. Okongwu, *Chem. Eng. J.*, **75**, 1 (1999).
22. A. Nouralishahi, H. Pahlavanzadeh and J. Towfighi Daryan, *Fuel Process. Technol.*, **89**, 667 (2008).
23. Z. Stansch, *Kinetics for oxidative coupling of methane over La_2O_3/CaO catalyst*, Ph.D Theses, Ruher University Bochum, Bochum (1997).
24. G. Chiappetta, G. Clarizia and E. Drioli, *Chem. Eng. J.*, **136**, 373 (2008).
25. I. Karafyllis and P. Daoutidis, *Comput. Chem. Eng.*, **26**, 1087 (2002).
26. M. Daneshpayeh, A. A. Khodadadi, N. Mostoufi, Y. Mortazavi, R. Sotudeh-Gharebagh and A. Talebizadeh, *Fuel Process. Technol.*, **90**, 403 (2009).
27. Z. Stansch, Z. Mleczko and M. Baerns, *Ind. Eng. Chem. Res.*, **36**, 2568 (1997).
29. J. Santamaria, M. Menendez, J. Pena and A. Barahona, *Catal. Today*, **13**, 353 (1992).
30. Y. K. Kao, L. Lei and Y. S. Lin, *Ind. Eng. Chem. Res.*, **36**, 3583 (1997).
31. I. P. Androulakis and S. C. Reyes, *AIChE J.*, **45**, 860 (1999).
32. Y. S. Su, J. Y. Ying and W. H. Green Jr., *J. Catal.*, **218**, 321 (2003).
33. M. Daneshpayeh, N. Mostoufi, A. A. Khodadadi, R. Sotudeh-Gharebagh and Y. Mortazavi, *Energy Fuel*, **23**, 3745 (2009).